

Supporting information

In-situ Etching-induced Self-assembly of Metal Clusters Decorated One-dimensional Semiconductor for Solar-powered Water Splitting: Unraveling Cooperative Synergy by Photoelectrochemical Investigations

Fang-Xing Xiao,^{a} Bin Liu^{b*}*

a. College of Materials Science and Engineering, Fuzhou, Fuzhou University.

b. School of Chemical and Biomedical Engineering, Nanyang Technological University, 62
Nanyang Drive, Singapore 637459, Singapore. Fax: (65) 6794-7553; Tel: (65) 6513-7971;

E-mail: fx Xiao@fzu.edu.cn
liubin@ntu.edu.sg

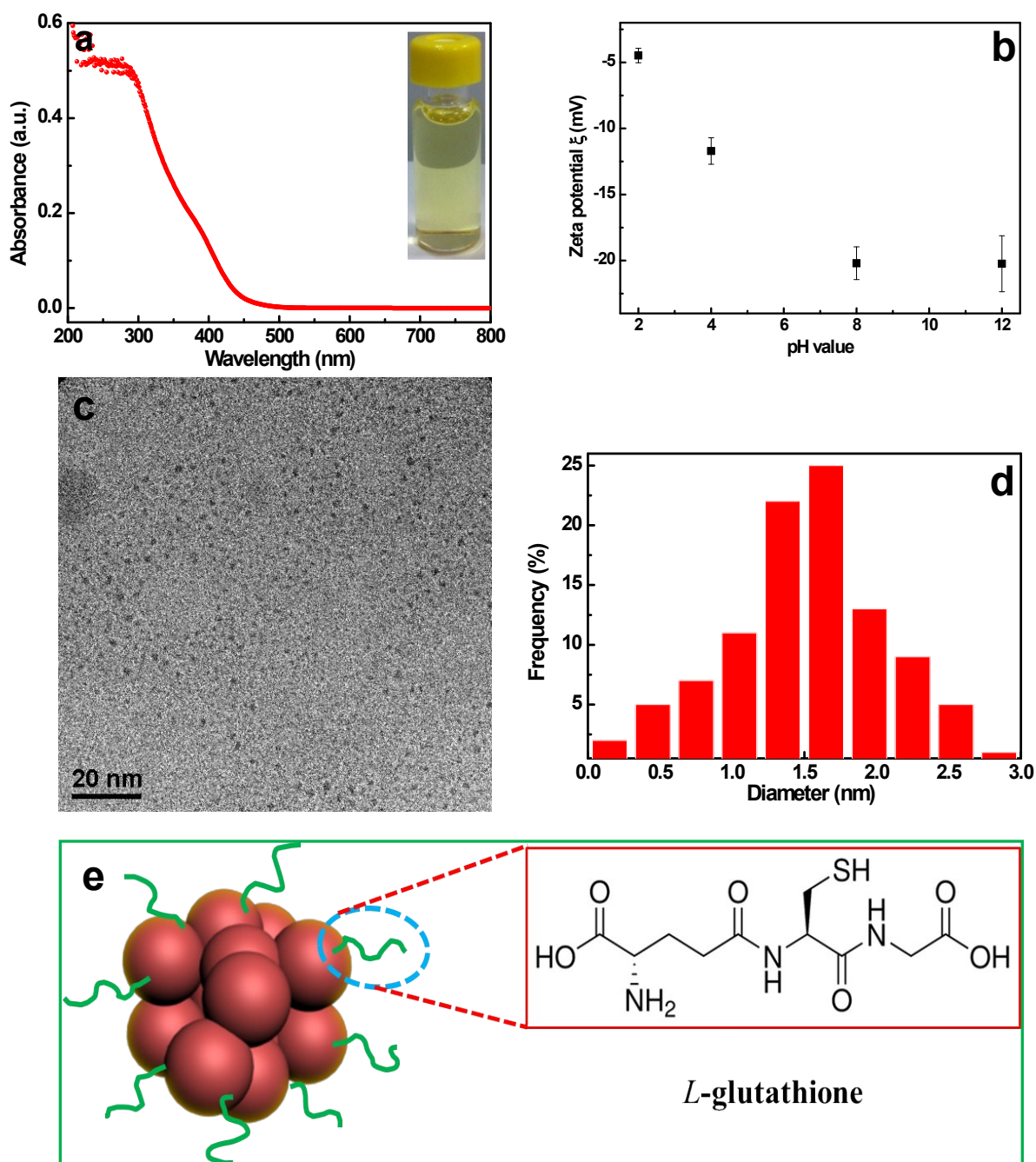


Fig. S1. (a) UV-vis absorption spectrum with corresponding photograph in the inset, (b) zeta-potential, (c) TEM image and (d) mean size distribution histogram of GSH-capped Au_x clusters; (e) schematic illustration depicting the molecule structures of Au_x clusters and surface ligand (GSH).

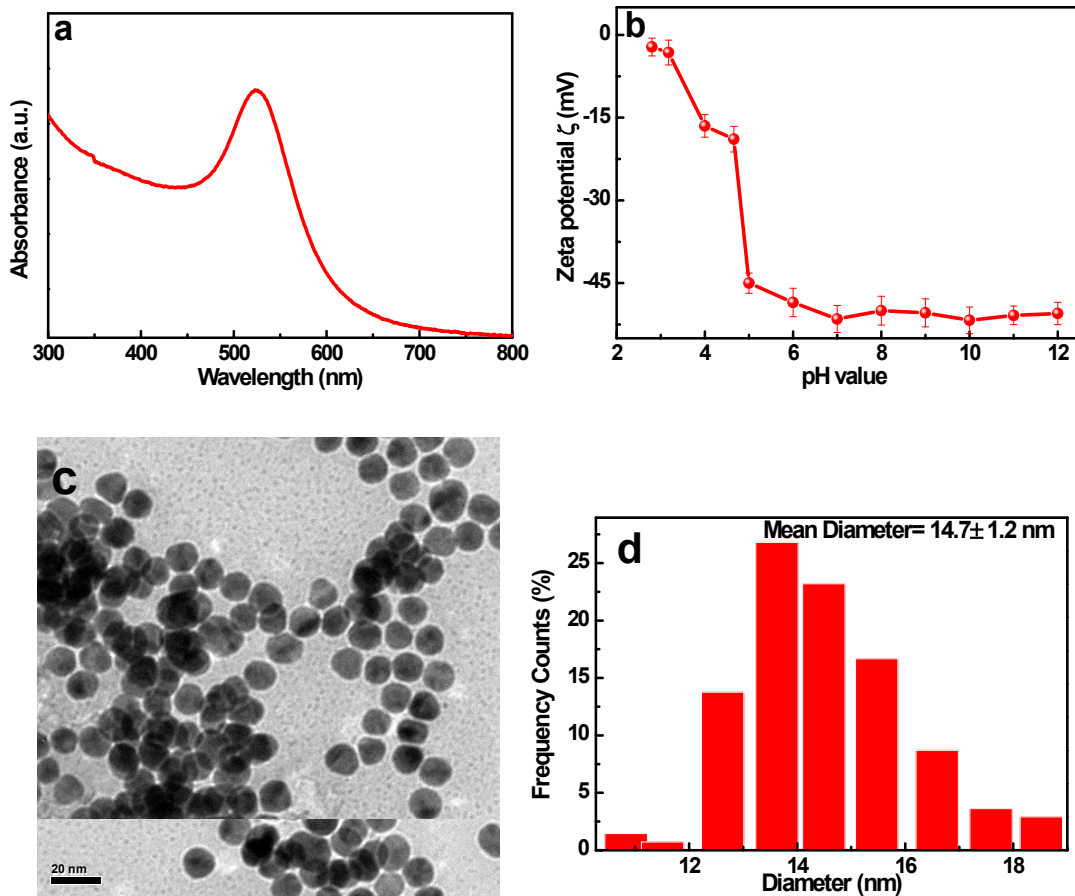


Fig. S2. (a) UV-vis absorption spectrum with corresponding photograph in the inset, (b) zeta-potential, (c) TEM images and (d) mean size distribution histogram of citrate-capped Au NPs.

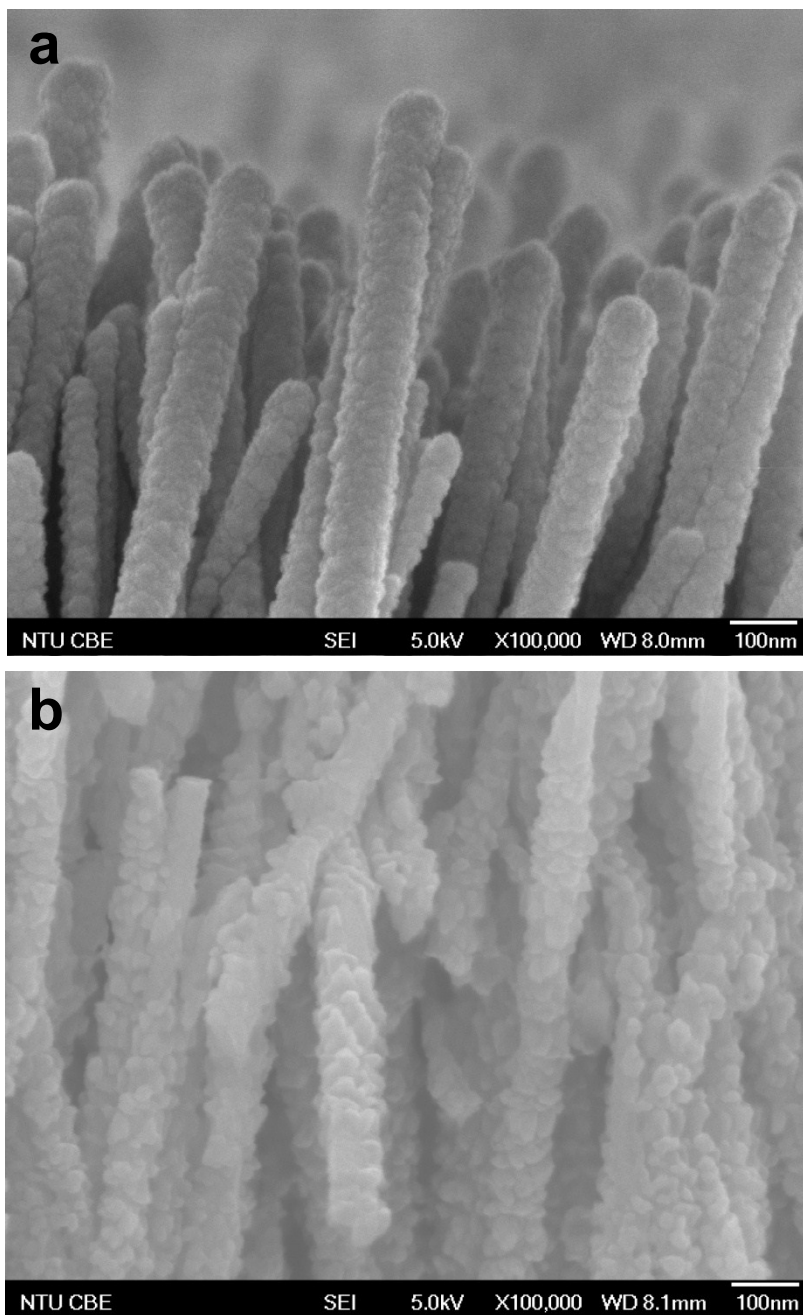


Fig. S3. High-magnified cross-sectional FESEM images of Au_x/ZnO NWs heterostructure on the (a) top and (b) at the bottom.

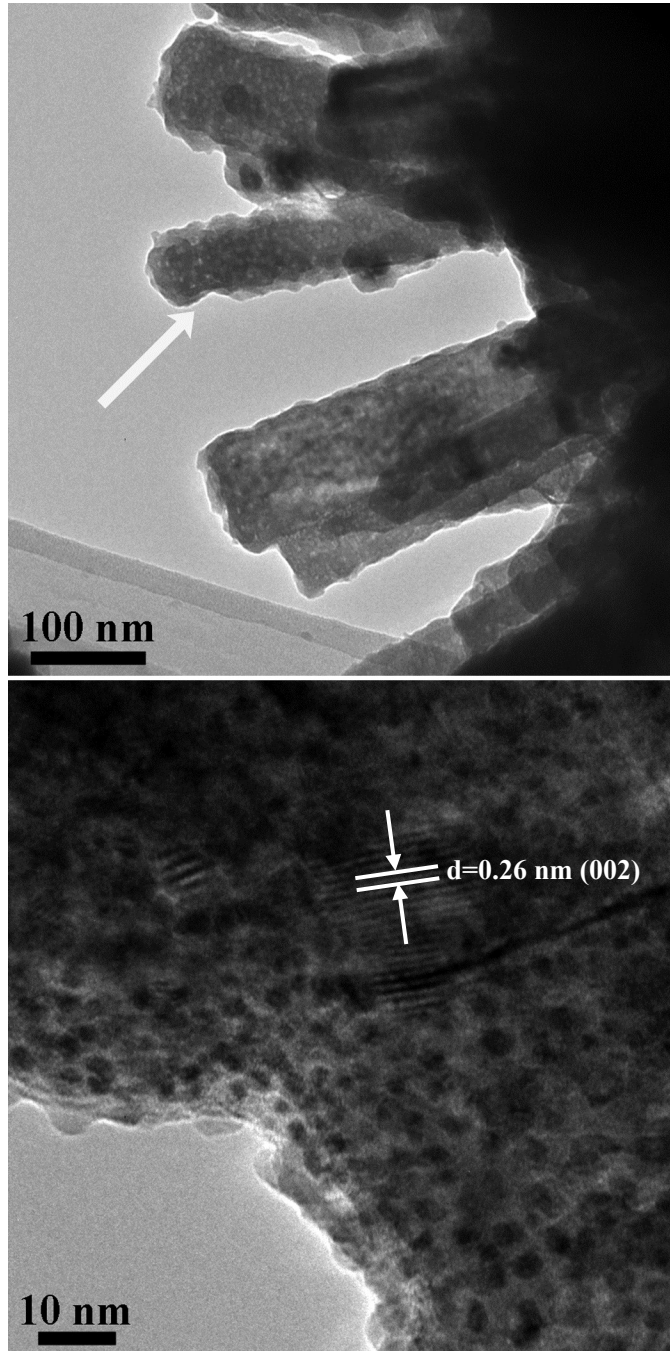


Fig. S4. HRTEM images of Au_x/ZnO NWs heterostructures.

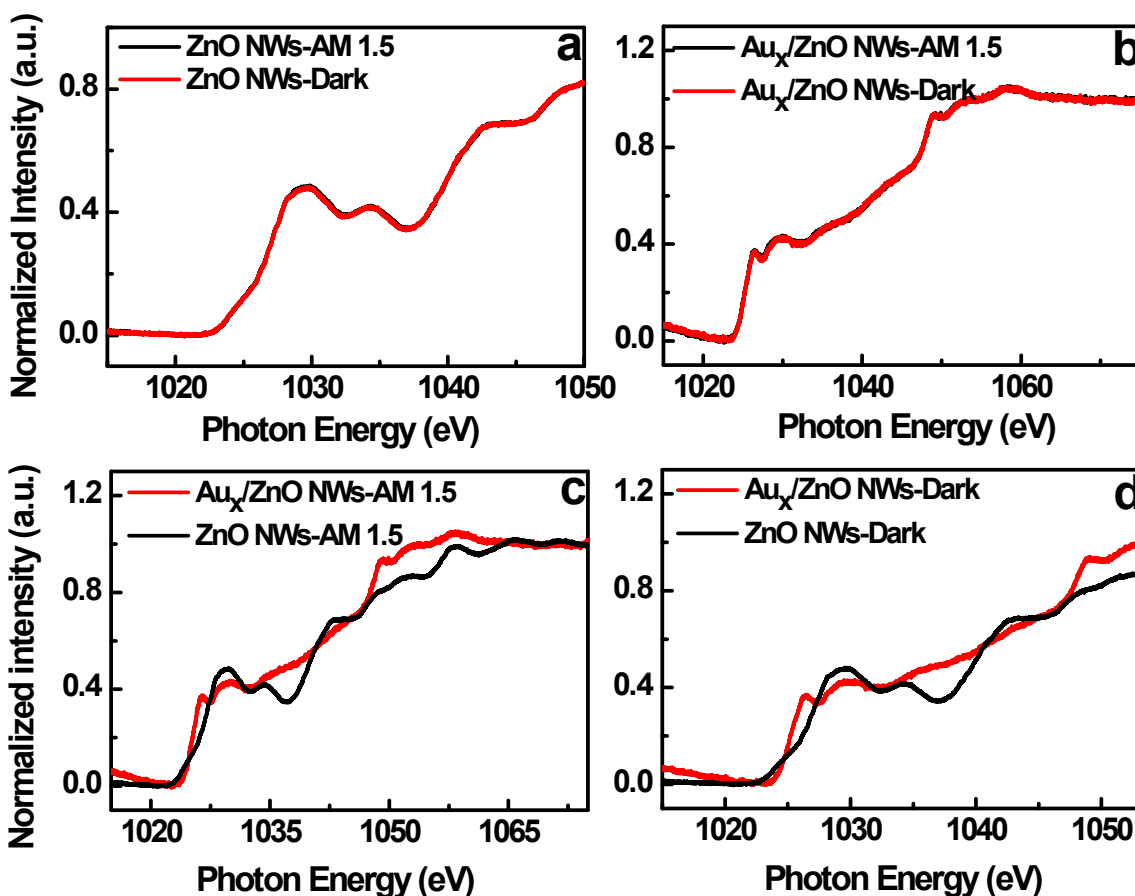


Fig. S5. X-ray absorption spectra (XAS) of Zn L-edge for (a) ZnO NWs and (b) Au_x/ZnO NWs heterostructure under simulated solar light (AM 1.5G) irradiation and in the dark. Comparison on the XAS results of Zn L-edge for ZnO NWs and Au_x/ZnO NWs heterostructure (c) under simulated solar light (AM 1.5G) irradiation and (d) in the dark.

Note: As shown in **Fig. S5**, negligible difference was observed in the XAS results of Zn L-edge for ZnO NWs and Au_x/ZnO NWs heterostructure under simulated solar light irradiation and in the dark. On the contrary, XAS result of Au_x/ZnO NWs heterostructure is different from ZnO NWs under the same simulated solar light irradiation or in the dark, with some characteristic peaks of ZnO shielded or substantially shifted, verifying the pronounced interaction between Au_x clusters and ZnO NWs framework afforded by electrostatic self-assembly.

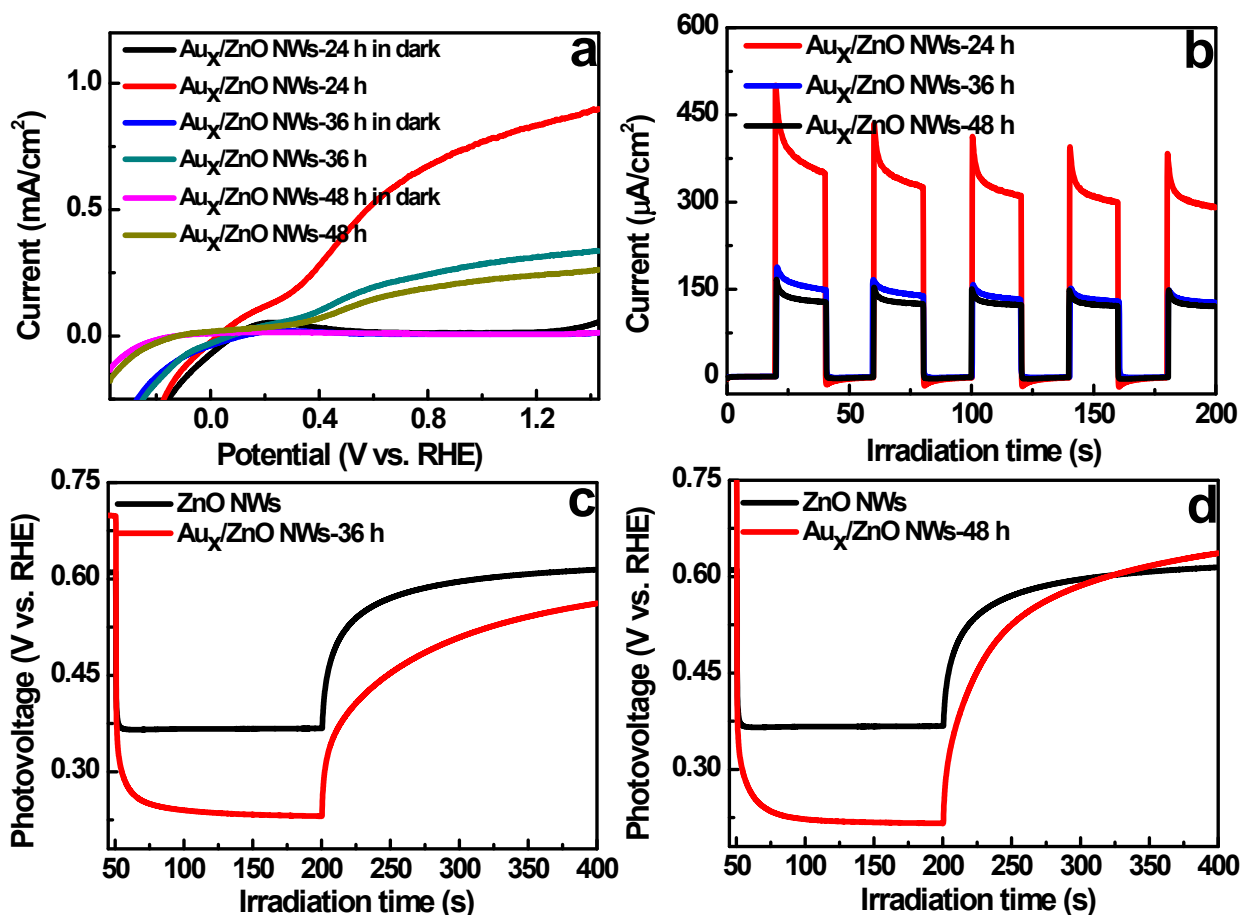


Fig. S6. (a) LSV plots and (b) on-off transient photocurrent responses of Au_x/ZnO NWs heterostructures with different dipping time in Au_x aqueous solution under simulated solar light irradiation (AM 1.5). Decay of photovoltage after on-off irradiation under simulated solar light irradiation (AM 1.5) for ZnO NWs and Au_x/ZnO NWs heterostructure with dipping time of (c) 36 h and (d) 48 h.

Note: Fig. S6 (a & b) show that photocurrent density of Au_x/ZnO NWs heterostructures with different dipping time in Au_x aqueous solution under simulated solar light irradiation follows the order of Au_x/ZnO NWs (t=24 h) > Au_x/ZnO NWs (t=36 h) > Au_x/ZnO NWs (t=48 h) > ZnO NWs, from which the optimal dipping time is 24 h. Moreover, as shown in Fig. S6 (c & d), Au_x/ZnO NWs (t=36, 48 h) heterostructures still demonstrated the much more prolonged electron lifetime in comparison with ZnO NWs under the same conditions.

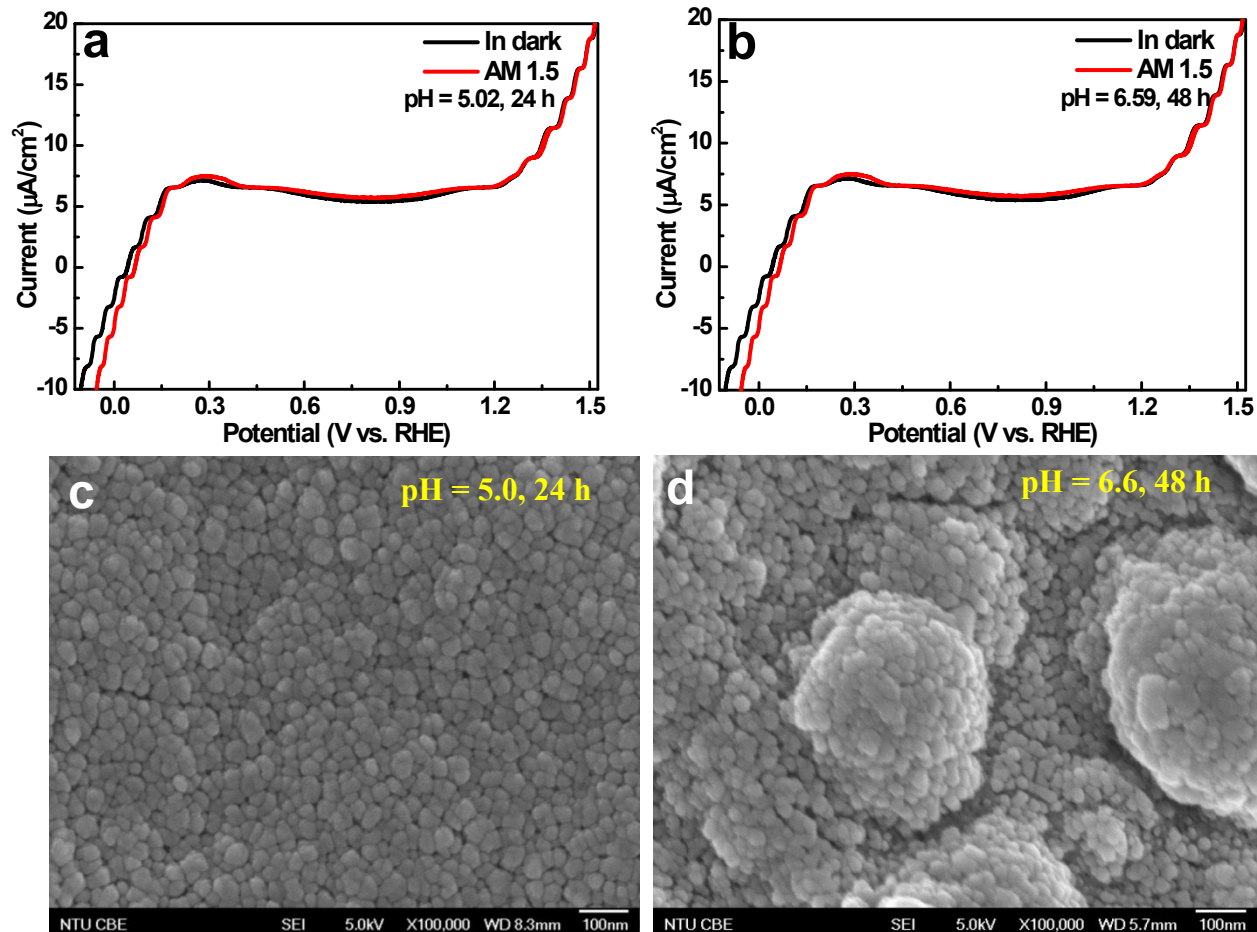


Fig. S7. LSV plots of Au_x/ZnO NWs heterostructures prepared by dipping ZnO NWs in Au_x clusters aqueous solutions with different pH values for different dipping time: (a) pH = 5.0, $t=24$ h, and (b) pH = 6.6, $t=48$ h under simulated solar light irradiation with corresponding FESEM images displayed in (c) and (d), respectively.

Note: As shown in **Fig. S7 (a & b)**, Au_x/ZnO NWs heterostructures prepared by dipping ZnO NWs into Au_x clusters aqueous solutions with pH values of 5.0 & 6.6 and dipping time of 24 & 48 h exhibited the negligible photocurrent under simulated solar light irradiation. The corresponding FESEM images in **Fig. S7(c & d)** show that 1D nanostructure of ZnO NWs matrix has been completely destroyed and it collapses to a large amount of small nanoparticles, thereby leading to the remarkably inferior PEC water splitting performances.

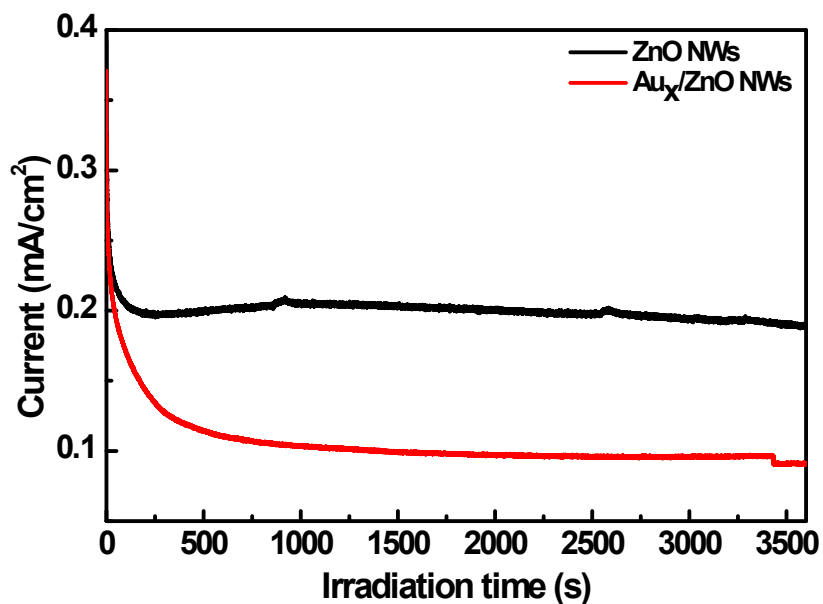


Fig. S8. I-t curves of ZnO NWs and Au_x/ZnO NWs heterostructure under continuous simulated solar light irradiation (bias 0.3 V vs. RHE, AM 1.5, 100 mW/cm²).

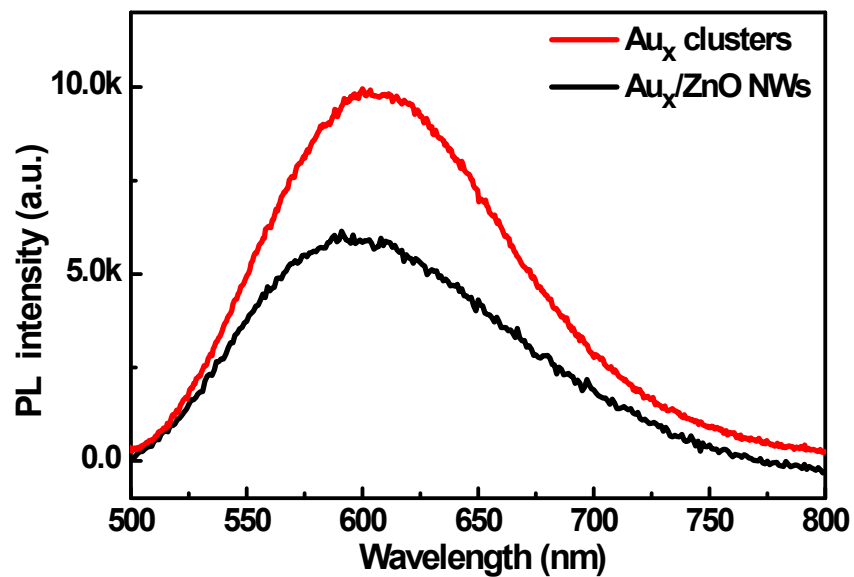


Fig. S9. PL spectra of Au_x clusters and Au_x/ZnO NWs heterostructure.

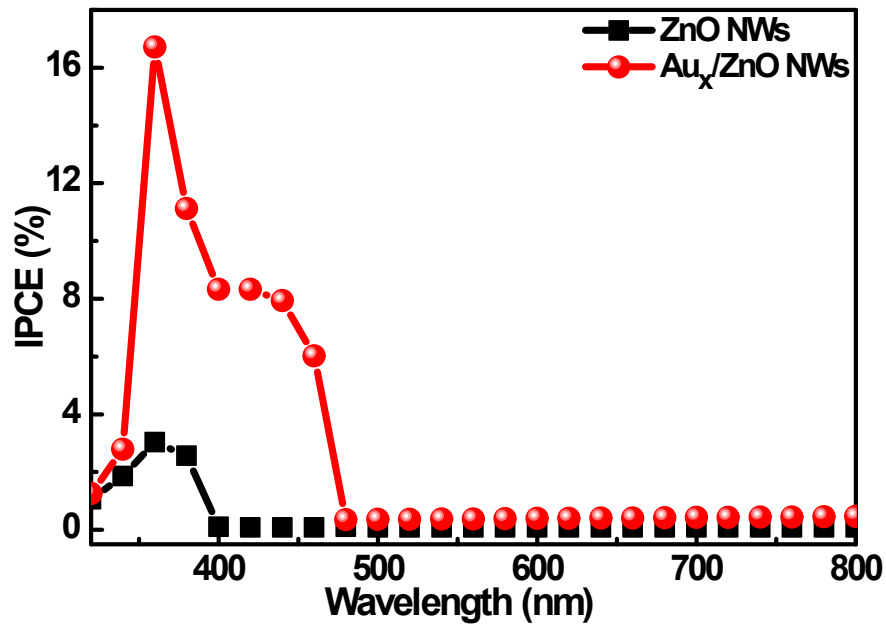


Fig. S10. Monochromatic incident photon-to-electron conversion efficiency (IPCE) spectra of pristine ZnO NWs and Au_x/ZnO NWs heterostructure.

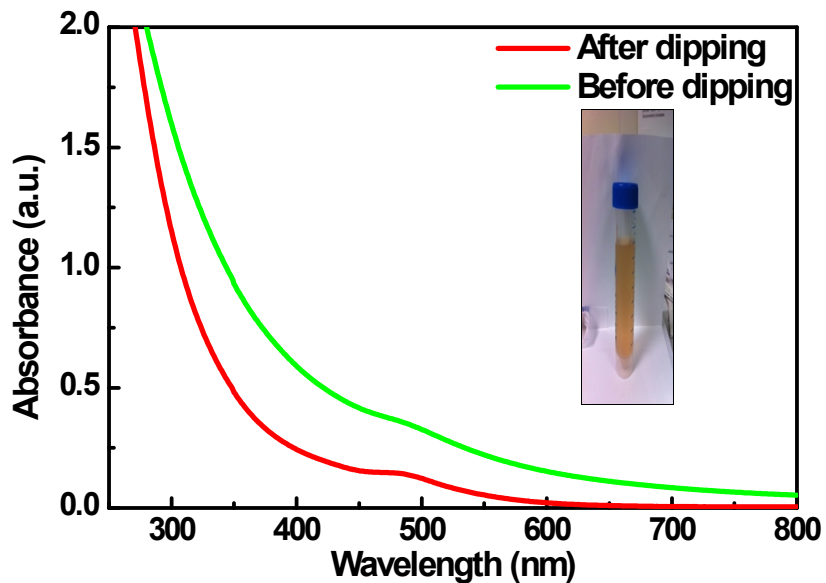


Fig. S11. UV-vis absorption spectra of Ag_x@GSH clusters aqueous solutions before and after ZnO NWs dipping for 24 h.

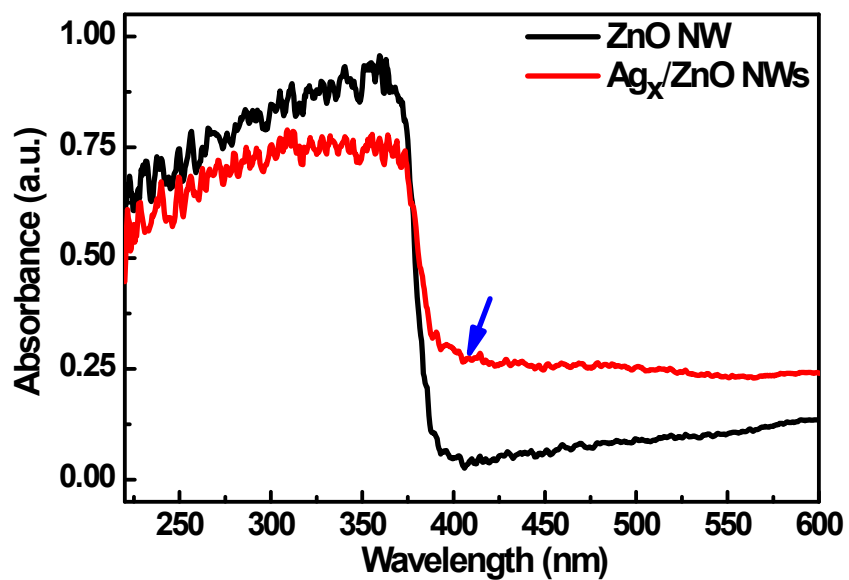


Fig. S12. UV-vis diffuse reflectance spectra of ZnO NWs and Ag_x/ZnO NWs heterostructure.

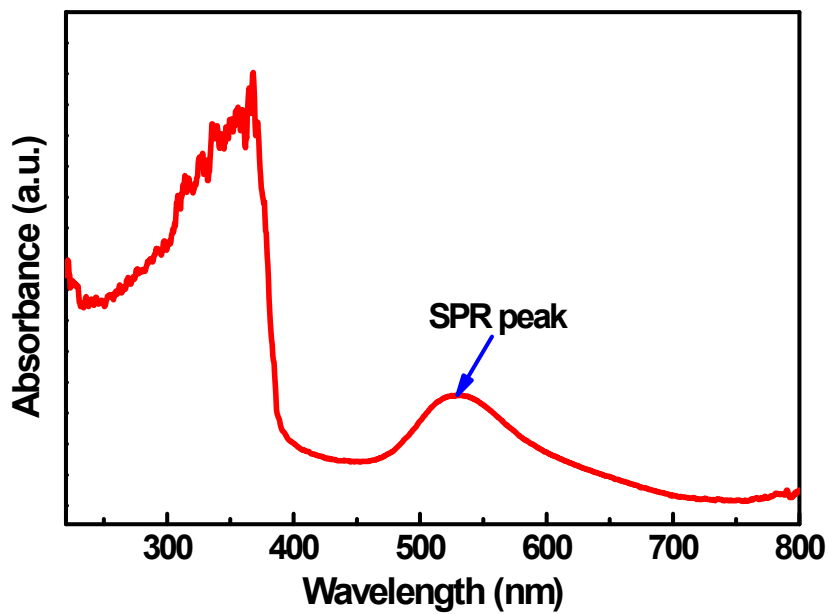


Fig. S13. UV-vis diffuse reflectance spectrum of Au NPs/ZnO NWs heterostructure.

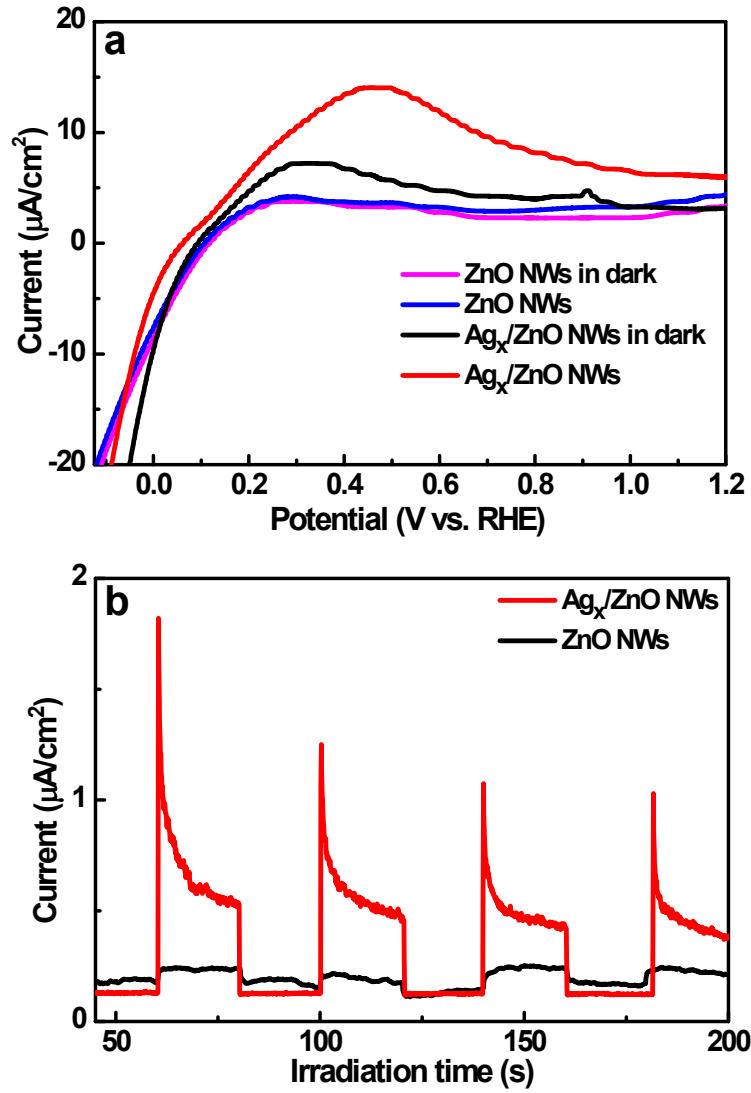


Fig. S14. (a) LSV plots and (b) on-off transient photocurrent responses of ZnO NWs and Ag_x/ZnO NWs heterostructure under visible light irradiation ($\lambda > 420$ nm).

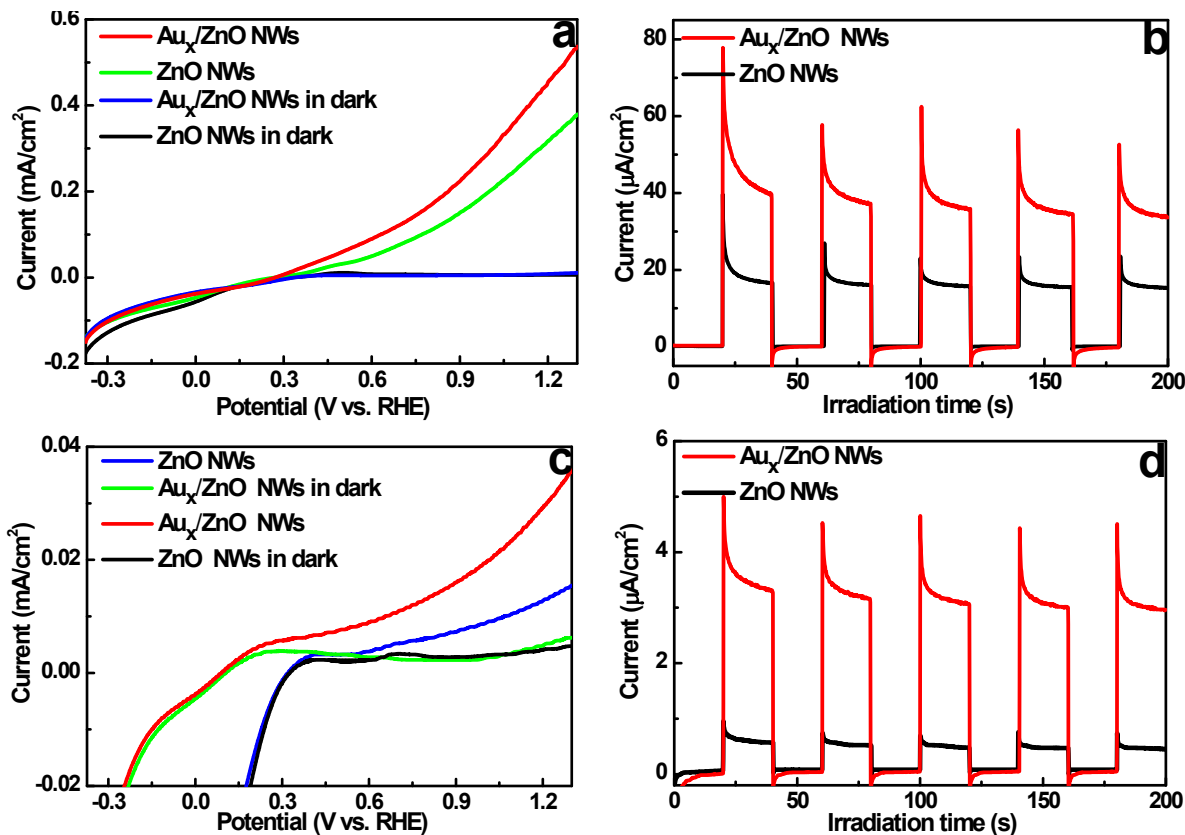


Fig. S15. LSV plots and on-off transient photocurrent responses of Au_x/ZnO NWs heterostructure in which ZnO NWs substrate was prepared by an electrodeposition method under (a & b) simulated solar light and (c & d) visible light irradiation ($\lambda > 420$ nm), respectively.

Note: Au_x/ZnO NWs heterostructure in which ZnO NWs substrate was prepared by an electrodeposition method still demonstrates significantly enhanced PEC water splitting performances in comparison with pristine ZnO NWs counterpart under both simulated solar and visible light irradiation, implying the vital role of Au_x clusters as photosensitizer was undoubtedly ascertained regardless of the properties of the semiconductor matrix used. Noteworthy, onset potential of Au_x/ZnO NWs was remarkably blue-shifted under visible light irradiation and this also substantiates the contribution role of Au_x clusters.

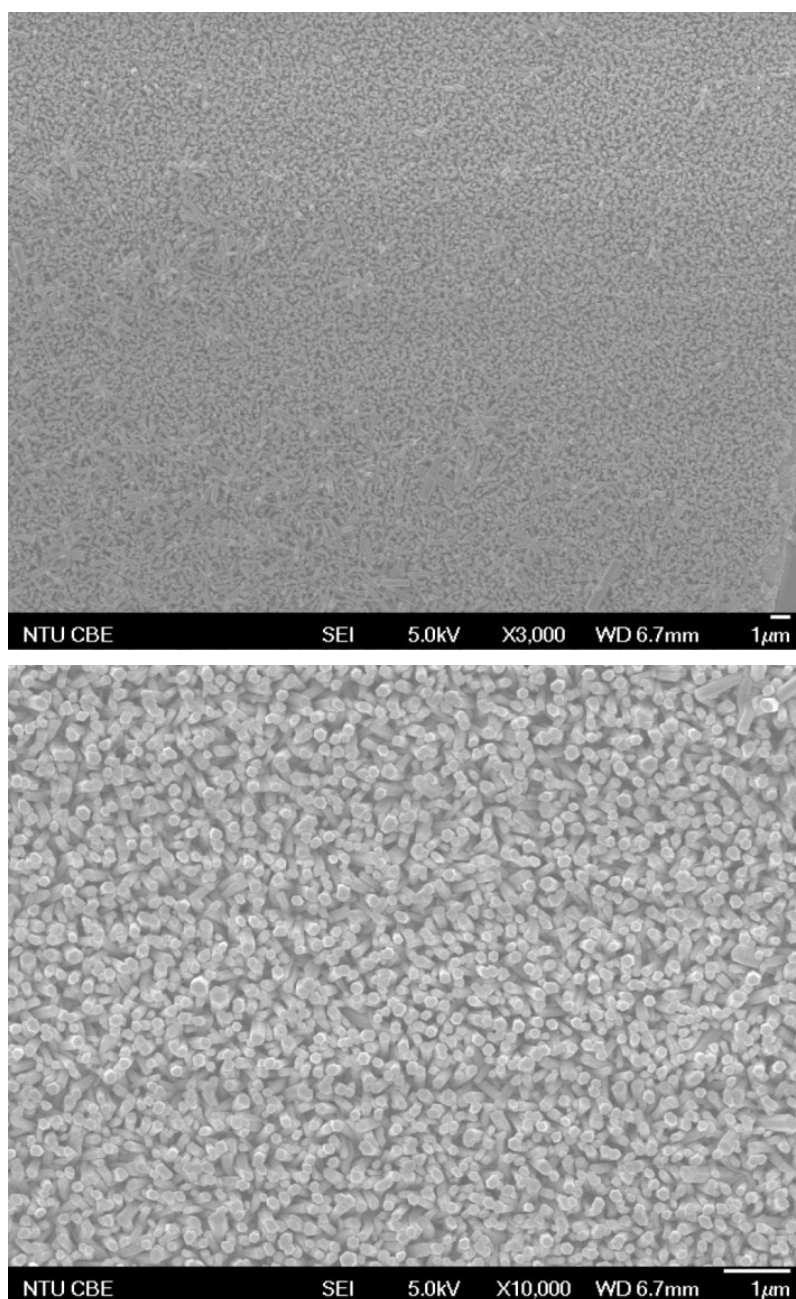


Fig. S16. FESEM images of ZnO NWs substrate prepared by an electrodeposition method.

Note: It is apparent that the morphology of ZnO NWs substrate prepared by an electrodeposition method is nearly the same to ZnO NWs substrate prepared via a solvent growth method, albeit both of which involve the similar seed deposition and growth process.

Table S1. Binding energy vs chemical bond species for Au_x/ZnO NWs heterostructure and ZnO NWs.

<i>Element</i>	<i>Au_x/ZnO NWs vs ZnO NWs (eV)</i>	<i>Chemical Bond Species</i>
C 1s A	284.60/284.60	C-C/C-H
C 1s B	285.88/286.28	C-OH/C-O-C ¹
C 1s C	287.38/N.A.	C-N ⁶
C 1s D	288.78/288.68	-COO ⁻ /Carboxylate (CO ₃ ²⁻) ²
O 1s A	531.13/529.95	Lattice oxygen (Zn-O)
O 1s B	532.61/531.63	Surface hydroxyl (Zn-OH) ³
O 1s C	533.75/N.A.	-COOH ⁴
Zn 2p _{3/2}	1021.71/1021.21	Zn ^{2+ 5}
Zn 2p _{1/2}	1044.78/1044.30	Zn ²⁺
Au 4f _{7/2}	83.75/83.75 (TiO ₂ /Au _x)	Metallic Au (0) ⁷
Au 4f _{7/2}	85.18/84.85 (TiO ₂ /Au _x)	Au (+) ⁸

Experimental section

Electrochemical deposition of ZnO NWs is carried out by our previous work.⁹ Prior to the deposition of ZnO NWs, FTO coated glass substrates were cleaned with detergent under sonication for 90 min, followed by washing with DI water. Then, ZnO NWs were deposited onto the pre-cleaned FTO-coated glass substrates using an electrochemical approach. The deposition of ZnO NWs was carried out in a 50 mL three-chambered electrochemical cell. 40 mL of aqueous solution containing 5 mM $\text{Zn}(\text{NO}_3)_2$ and 50 mM NaNO_3 (pH = 9) was used as the electrolyte, and the temperature was kept at 85 °C in a hot water bath. Pre-cleaned FTO-coated glass, platinum (Pt) foil and saturated calomel electrode (SCE) were used as the working, counter and reference electrodes, respectively. The ZnO NWs were deposited onto FTO-coated glass substrates using a multi-potential step technique. A ZnO seed-layer was first deposited on FTO with a potential of -1.3 V vs. SCE for 10 seconds. Therefore, a constant potential of -1.0 V vs. SCE was applied for 2000 seconds. After the deposition, the as-prepared films were rinsed with DI water, dried with compressed N_2 flow and then annealed at 350 °C in air.

References

1. S. Biniak, G. Szymanski, J. Siedlewski and A. Swiatkowski, *Carbon* 1997, **35**, 1799-1810.
2. X. M. Wei and H. C. Zeng, *Chem. Mater.* 2003, **15**, 433-442.
3. J. Li, S. B. Tang, L. Lu and H. C. Zeng, *J. Am. Chem. Soc.* 2007, **129**, 9401-9409.
4. F. -X. Xiao, J. Miao, H. -Y. Wang and B. Liu, *J. Mater. Chem. A*, 2013, **1**, 12229-12238.
5. F. -X. Xiao, S. -F. Hung, H. Tao, J. Miao, H. B. Yang and B. Liu, *Nanoscale*, 2014, **6**, 14950-14961.
6. C. D. Wagner, W. M. Riggs, L. E. Davis, J. F. Moulder and G.E. Muilenberg, *Handbook of X-Ray Photoelectron Spectroscopy*, Perkin-Elmer, Eden Prairie, Minn, USA, 1979.
7. H. X. Li, Z. F. Bian, J. Zhu, Y. N. Huo, H. Li and Y. F. Lu, *J. Am. Chem. Soc.*, 2007, **129**, 4538-4539.
8. J. Huang, W. L. Dai and K. N. Fan, *J. Catal*, 2009, **266**, 228-235.
9. J. Miao, H. B. Yang, S. Y. Khoo, B. Liu, *Nanoscale*, 2013, **5**, 11118-11124.